Delay in timing and spatial reorganization of rainfall due to urbanization- analysis over India's smart city Bhubaneswar

Madhusmita Swain[1,2], Raghavendra Raju Nadimpalli[2,3], Uma Charan Mohanty[1], Pulak Guhathakurta[4], Akhilesh Gupta[5], Akshara Kaginalkar[6], Fei Chen[7] and Dev Niyogi[2,8*]

Abstract

Bhubaneswar is the first designed 'smart city' in India and has experienced rapid urbanization since 2000. The question undertaken in this study is to assess if there is a change in the rainfall over this rapidly urbanizing region, and if so, what are the characteristics of the change? The broader intent is to understand if the change in urbanization and rainfall are interlinked? The India Meteorological Department (hourly station and daily gridded) and Tropical Rainfall Measurement Mission (3-hourly) datasets are analyzed for the 1980–2018 period (39 years) for different seasons separately. Wavelet and trend analysis reveal that precipitation intensity has increased over the study period. The assessments of the hourly rainfall data show an interesting feature. There is a decrease in the midnight to early-morning rain, with a corresponding increase in the late-afternoon to midnight rainfall. The increase in the rainfall is preferentially downwind and on the east side of the city. A supervised classified land use land cover map of the Bhubaneswar region is developed for 1980, 1990, 2000, 2010, and 2019 using Landsat imagery to compute the urban sprawl. The urban area and population density over Bhubaneswar is increasing with time. Analysis of the LULC and rainfall data indicates that the rainfall over urban regions and the shift in the timing of rains to evenings is highly correlated with the urban sprawl.

Keywords Heavy rains, Urban climate, Urban sprawl, Land use land cover change, Pre-monsoon rains, Indian monsoon, Wavelet analysis, Rainfall modification

1 Introduction

Urbanization and regional climate change are major global environmental concerns (Solecki et al., 2013) and the two are interlinked (Pielke Sr et al., 2011). Urbanization manifests through the increase in the urban population and the expansion of impervious surface area. Since 1900, the proportion of the global urban population has increased from 13% to more than 50% (Seto & David, 2010). Urban sprawl alters local and regional meteorology- humidity, wind speed, temperature, and planetary boundary layer height (Arnfield, 2003). Urbanization also modifies the exchange of heat, moisture, aerosols, and momentum between the land surface and the overlying atmosphere. Consequently, urbanization directly influences the changing weather

*Correspondence:
Dev Niyogi
dev.niyogi@jsg.utexas.edu
[1] School of Earth, Ocean and Climate Sciences, Indian Institute
of Technology, Bhubaneswar, Odisha 752050, India
[2] Department of Agronomy, and Department of Earth, Atmospheric,
and Planetary Sciences, Purdue University, West Lafayette, IN 47907, USA
[3] India Meteorological Department, Delhi 110003, India
[4] India Meteorological Department, Pune, Maharashtra 411005, India
[5] SPLICE, Department of Science and Technology, New Delhi, India
[6] C-DAC, Pune, Maharashtra, India
[7] Research Application Laboratory, NCAR, Boulder, CO 80305, USA
[8] Department of Geological Sciences, Jackson School of Geosciences,
and Department of Civil, Environmental and Architectural Engineering,
Cockrell School of Engineering, The University of Texas, Austin, TX 78712,
USA

patterns over and around cities and impacts the community and economy (National Research Council, 2010).

In a recent meta-analysis review of urbanization studies, Liu and Niyogi (2019) conclude that there is an ongoing need for observational assessments related to the impact of urban landscapes on different weather parameters. Using a combination of modeling and observational datasets, studies have concluded that the changes in rainfall over a city are associated with an increase in urbanization of the city (e.g. Buishand, 1979; Shepherd et al., 2002; Burian & Shepherd, 2005; Chen et al., 2007; Liang et al., 2011; Zhang et al., 2019; Lorenz et al., 2019; Liu & Niyogi, 2019; Niyogi et al., 2020). The urban-rural heterogeneity strengthens mesoscale convection. Urbanization may suppress rainfall over the city and create conditions favorable for downward enhancement (Niyogi et al., 2011; Zhang et al., 2019; Wen et al., 2020). With the increase in built-up areas, urbanization generally modifies the regional atmospheric circulations, which results in more intense rainfall (Kumar et al. 2013). Studies such as Yang et al. (2017) report that short-lived extreme rainfall events are strongly associated with urbanization. Studies (Siswanto et al., 2016; Niyogi et al., 2020) also suggest a possible delay in late afternoon rainfall due to urbanization. Analysis of spatio-temporal variation of rainfall and urbanization reveals that urban areas with the highest population areas are dominated by the slightly longer rainfall duration and higher rainfall intensity (Zhu et al., 2019). There is also a significant correlation between the spatial distribution of heavy rainfall amount and an increase in urbanization over India (Kishtawal et al., 2010), the United States (Niyogi et al., 2017; Singh et al., 2020), and China (Zhi-Hong et al., 2016, and Shi et al., 2017).

Over the Indian monsoon region, Bisht et al. (2018) concluded that there is an increasing trend in pre-monsoon season rainfall over most parts of India during the post-urbanization era (1971–2015) compared to during the pre-urbanization era (1901–1970). Changes in urbanization are likely to significantly alter Indian Monsoon Rainfall (IMR) and cause extreme rainfall over the various urban regions (Kishtawal et al., 2010; Dimri and Niyogi 2013; and Singh et al., 2016). This study is focused on the rapidly urbanizing Indian city of Bhubaneswar, the capital of Odisha state along the Bay of Bengal. The city is designated as the first 'smart city' being developed in India (Bhattacharya et al., 2015). The remarkable urbanization rate experienced for Bhubaneswar has been studied in Pathy and Panda (2012), and the impact on temperature has been reported in Swain et al. (2017), Barik et al. (2019), and Gogoi et al. (2019). The city has

also experienced several heavy rainfall events that, according to long-term residents, appear to be on the rise.

The study's main goal is to determine whether the rainfall in Bhubaneswar, which is quickly urbanizing, has changed and, if so, what the characteristics of that change are. The overarching goal is to determine whether urbanization change and rainfall variation are connected. Pre-monsoon (March–April–May: MAM), monsoon (Jun–Jul–Aug–Sept: JJAS), post-monsoon (Oct–Nov–Dec: OND), and winter (Jan – Feb: JF) are some of the seasons with interest in terms of rainfall characteristics. The investigation is driven by its possible effects on managing flash floods, mudflows, and waterlogging in metropolitan areas.

2 Data and methods
This section describes the datasets and methodology used to carry out the present research work.

2.1 Study area
Bhubaneswar (centered at 85.84° E and 20.27° N and 45 m above sea level, is a prominent city on the eastern coast of India Fig. 1(a)). Bhubaneswar is located in Khordha district, surrounded by Cuttack on its north, Nayagarh on the west, Puri on its south, and Jagatsinghpur on the east. The extended map of the city with surface relief is shown in Fig. 1(b). The color maps show that there are about 21 different land use land cover (LULC) classes. Bhubaneswar is one of the fastest-growing urban areas in the country, and a designated 'smart city'. The city has also experienced frequent natural hazards such as heatwaves, tropical cyclones, and flooding (Mohanty et al., 2013; Panda et al., 2014; Gupta, 2020). The city experiences a humid sub-tropical climate with World Meteorological Organization (WMO) code 42971. Climatologically, the average annual temperature is 27.4 °C, and annual rainfall is about 1505 mm. The maximum temperature is observed during pre-monsoon season (MAM), and maximum precipitation is observed during the July & August month of the year over the city (Pandey et al., 2014). The city has grown from a population of 8170 in 1921 to 881,988 in 2011 (Census of India, Odisha State, 2011). It has been projected for 2021 year and which is about 2150, 000 (Thandar, 2012). Bhubaneswar city area is characterized by undulating upland topography in western and central part while the eastern part is relatively flat with gentle slope. The main drainage channel is the Kuakhai River which is a distributary of the Mahanadi River. The soils are mainly Alfisols and Ultisols (Choudhury et al., 2011).
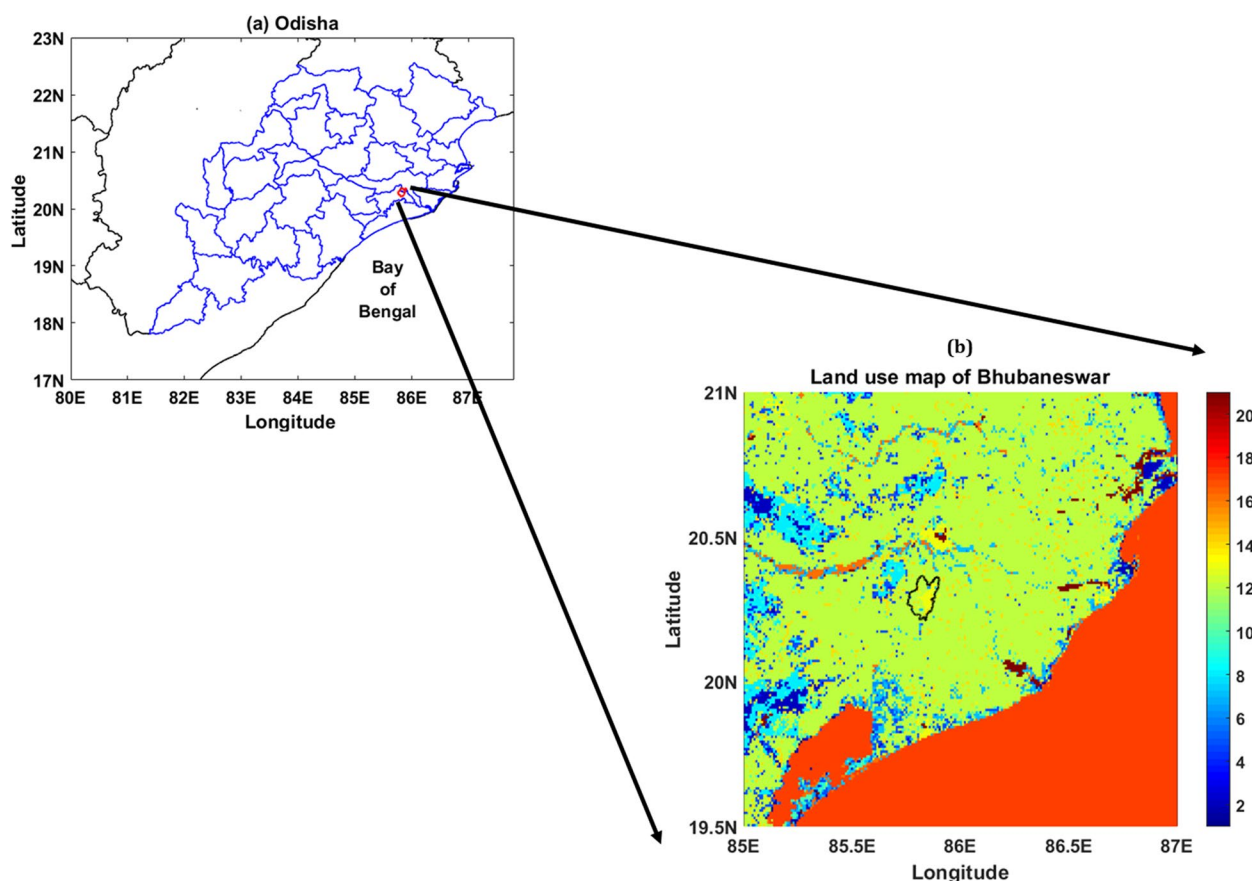
Fig. 1 Study area showing (**a**) the east coast state of Odisha and the location of the capital city Bhubaneswar; **b** municipal boundary of the city, with the numbers indicating the landmarks across Bhubaneswar city (names are in the table shown left side to the image) discussed in the text

2.2 Data used

The spatio-temporal characteristics of rainfall during four different seasons over Bhubaneswar station are analyzed using quality-controlled hourly rainfall data obtained from the National Data Centre (NDC) of India Meteorological Department (IMD), Pune. For the 39 years (1980–2018) of the study period, there are 49 days of missing data for Bhubaneswar. The gridded daily rainfall analysis obtained from the IMD (Pai et al., 2014) at a horizontal resolution of 0.25° × 0.25° is used in addition to the station data. The study period is confined to the recent era of 39 years (1980–2018) since more automated weather station data was used to generate the gridded rainfall analysis using the WMO standard quality control method. To supplement the IMD observations, three-hourly rainfall data at a horizontal resolution of 0.25° × 0.25° for the 1999–2018 year (depending on the availability of data) from Tropical Rainfall Measuring Mission (TRMM) has been used (Huffman et al., 2015). To assess the urbanization changes, cloud-free images from United States Geological Survey (USGS) Landsat satellite for 1980, 1990,

2000, 2010, and 2019 were acquired (https://landsat.gsfc.nasa.gov). These were used for supervised classification, and a summary is shown in Table 1 (Barsi et al., 2007; Dewan & Yamaguchi, 2009). Population density data for Bhubaneswar city has been taken from Socio-Economic Data and Applications Center (SEDAC) for 2000, 2010, and 2020 year (Center for International Earth Science Information Network (CIESIN), Columbia University, 2018).

2.3 Methodology used

Rainfall for different seasons over Bhubaneswar has been studied by using both hourly and yearly trend analysis. In addition, both parametric and non-parametric statistical methods have been used to detect trends and other changes in climate variables and are discussed in the following section (Suhaila & Jemain, 2009, and Jha & Singh, 2013). Methodology used in this recent study has been shown in Fig. 2. To investigate trend yearly and hourly rainfall over Bhubaneswar both Continuous Wavelet Transform (CWT) technique and

Table 1 Details of Landsat Satellite data processed for the urban land use/cover analysis

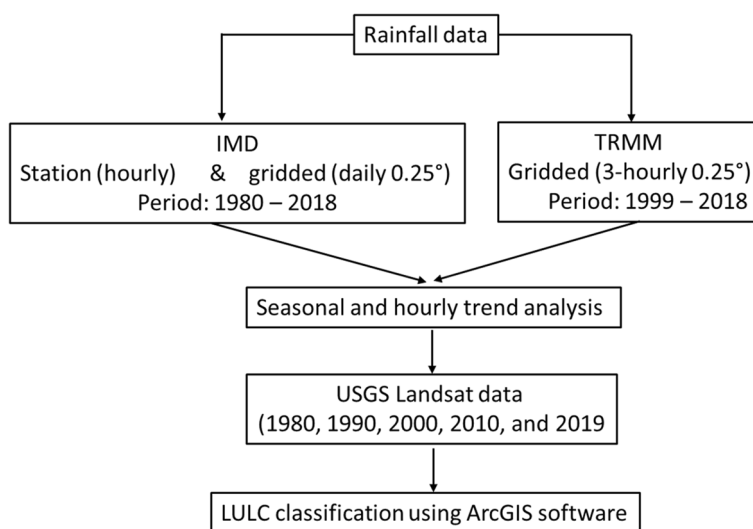| Sensor	Date of acquisition (Path/Row)	Data Type and bands
Multispectral Scanner System (MSS)	18 Jan 1980 (140/46)	Digital (4, 5, 6, 7)
Thermal Mapper (TM)	15 Mar 1989 (139/46) 28 Jan 1990 (140/46)	Digital (1, 2, 3, 4, 5, 6, 7)
TM	07 Dec 1999 (140/46) 02 Dec 2000 (139/46)	Digital (1, 2, 3, 4, 5, 6, 7)
TM	04 Feb 2010 (140/46) 13 Feb 2010 (139/46)	Digital (1, 2, 3, 4, 5, 6, 7)
TM	05 Jan 2019 (139/46) 12 Jan 2019 (140/46)	Digital (1, 2, 3, 4, 5, 6, 7, 8, 9, 10, 11)

Fig. 2 Flowchart of methodology used

the Mann-Kendall trend tests have been carried out. First, the possible existence of significant autocorrelations in the used datasets have been checked.

2.3.1 Mann-Kendall significant test

The non-parametric Mann-Kendall (MK) method has been widely used in recent years for climatic time series analysis (Mann, 1945; Kendall, 1948; Yue et al., 2003; Singh et al., 2008). In this study, the MK test has been used to verify the confidence in the trend analysis. This was calculated using MATLAB 2017a. The advantages of using the MK test are that (i) it is distribution independent and suitable for data with missing or censoring values, (ii) it has high asymptotic efficiency (Berryman et al., 1988; Fu et al., 2004; Modarres & Sarhadi, 2009), and (iii) the test is not affected by gross data errors and outliers. The *p*-value of the test generally defines the significance of the trend. Lesser than threshold *p*-values suggest rejection of the null hypothesis.

The significant test has been applied to an annual maximum rainfall time series x_i ranked from $i = 1...., n - 1$, and x_j is ranked from $j = i + 1, ..., n$. Each data point x_i is used as a reference point and is compared with all other data point x_j such that

$$sgn\ (x) = \begin{cases} 1, & when\ x_j > x_i \\ 0, & when\ x_j = x_i \\ -1 & when\ x_j < x_i \end{cases} \quad (1)$$

Kendall statistics (S) is defined as follows,

$$S = \sum_{i=1}^{N-1} \sum_{j=i+1}^{N} sgn\ (x_j - x_i) \quad (2)$$

Where "N" represents the length of the data series.

The variance is defined as,

$$Var(S) = \frac{1}{18} \left\{ n(n-1)(2n+5) - \sum_{i=1}^{g} t_i\ (t_i - 1)(2t_i + 5) \right\} \quad (3)$$

Where 't$_i$' indicates the extend of ith tied groups (a set of sample data with similar values) number and 'g' denotes the tied groups number.

The value of (S) and Var (S) has been calculated to develop standardized test measurement of 'Z' and which is as follows.

$$Z = \begin{cases} \frac{S-1}{\sqrt{\mathrm{var}(S)}}, & when\ S > 0 \\ 0, & when\ S = 0 \\ \frac{S+1}{\sqrt{\mathrm{var}(S)}}, & when\ S < 0 \end{cases} \quad (4)$$

Positive values of Z-statistics depict increasing, while the negative values indicate a decreasing trend in the time series. Statistics of MK test is based on the '+' or '-' signs; so the trends obtained from MK test are less affected by the outliers and the non-parametric MK test is beneficial for such data (Helsel & Hirsch, 1992, and Birsan et al., 2005).

2.3.2 Wavelet analysis

The wavelet transform (WT) is the other statistical approach used in this study. It is a mathematical technique for analyzing the data in a broad spectrum of time-frequency. A WT mathematically decompose a signal into multiple lower resolution levels. Among several mathematical transformations, Fourier transforms are the most popular (Santos et al., 2003). This analysis simultaneously provides both a time and frequency view of one-dimensional time series. The amplitude and time variation of such amplitude of any time series data can be obtained (Torrence & Compo, 1998). Wavelet analysis is a widely used method to detect different parameters periodic variation on different time scales (Weng & Lau, 1994, and Ling et al., 2012). The wavelet transforms analysis is effective in analyzing non-stationary time series and capturing useful information from it (Wei et al., 2012, and Adarsh & Reddy, 2015). The continuous wavelet transform shows a time-scale representation of the signal and helps analyze long-period datasets (Meyers et al., 1993; Wang & Wang, 1996).

Early applications of wavelet analysis include ocean waves, El Nino-Southern Oscillation, and turbulence (Wang & Wang, 1996). However, wavelet aided methods have been widely used in precipitation data to detect trends (Partal & Küçük, 2006; Sang, 2013; Shiau & Chiu, 2019; Pal et al., 2019). In recent years, wavelet analysis has been an effective approach for studying extreme precipitation (Kumar, 1996; Wang et al., 2013; Tan et al., 2016; Rathinasamy et al., 2019).

For a wavelet function ' φ ', the time-scale continuous wavelet transform (CWT) is defined as (Daubechies, 1990),

$$W(a, \tau) = \frac{1}{\sqrt{|a|}} \int_{-\infty}^{\infty} f(t)\varphi\left(\frac{t - \tau}{a}\right) dt \quad (5)$$

Where 't' is the time, 'a' and ' τ 'are the scale and location parameters. The CWT equation represents the signal (t); where the original signal can be reconstructed with the minimum of W(a, τ). The cone of influence (COI) is the area of the wavelet power spectrum where edge effects cannot be ignored (Gu et al., 2020).

2.4 Land cover classification

For developing the land cover change assessment, cloud – free imageries for Bhubaneswar city have been acquired from United States Geological Survey (USGS) Landsat satellite datasets. The sampling corresponding to five different years: 1980, 1990, 2000, 2010, and 2019 (Table 1) was analyzed. ArcGIS 10.2 has been used to digitalize the image and create a GIS database. Initially, Landsat imageries were formatted to the World Geodetic System (WGS84) reference datum and zone 43 north projection of Universal Transverse Mercator (UTM) system. Three follow up steps are involved for satellite image interpretation such as image pre-processing, processing, and post-processing, and were undertaken next.

The flowchart of the methodology followed for the generation of built-up area maps is presented in the Fig. 3. Preprocessing of image includes geometric corrections, radiometric calibration of the image data and filtering of noise present in the data. As a part of image processing, false color composite (FCC) images have been created using red, green, and near infrared channels.

Red areas present in the FCC have been interpreted as vegetation, black color areas as deep water, white color as barren land, and cyan color as urban built-up area, respectively. Variation of color tones for urban area vary with density and material use. Multispectral images were captured by stacking several bands of the image in FCC for each year separately. For 1990, 2000, 2010, and 2019, two Landsat scenes from paths 139 and 140 have been mosaiced to visualize the image as per landuse using ArcGIS. Row refers to the latitudinal center line of a frame of the imagery taken by the satellite. Satellite moves along its path, and the instruments present in the satellite scans the earth surface.

A supervised classification methodology (Jain et al., 2016; Swain et al., 2017; Barik et al., 2019) is used to produce LULC maps for Bhubaneswar city. The raster image is then classified into eight classes (urban built up, water, wetland, barren land, broadleaf deciduous forest, mixed forest, shrub/grass, and irrigated cropland). In supervised classification, the user develops the spectral signatures for different land use categories and then the ArcGIS software help assign the other pixels of
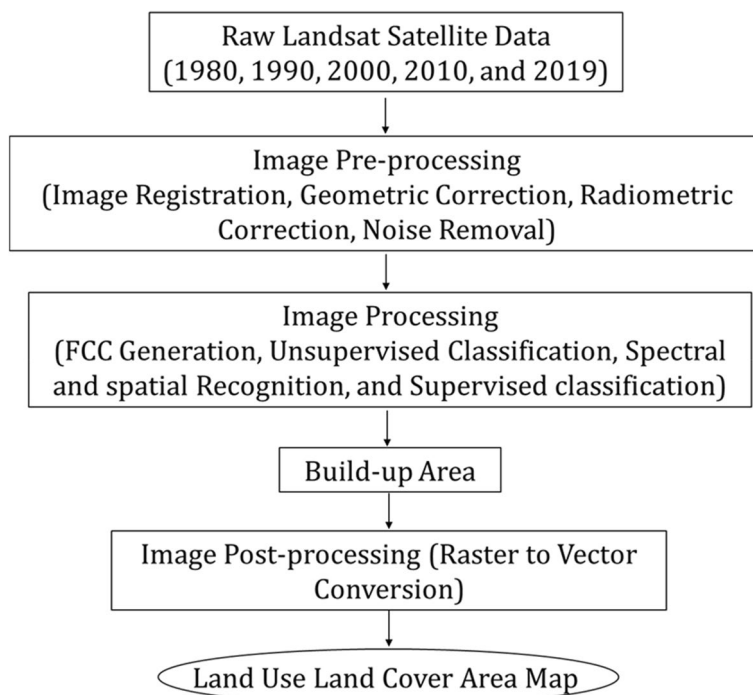
Swain *et al. Computational Urban Science*   (2023) 3:8

Page 6 of 14

Fig. 3 Flowchart of methodology used for LULC generation

the same signature into one class (Eastman, 2003). This process is frequently used in remote sensing for quantile analysis of datasets. In supervised classification, the first step is to define the training site i.e., area of interest. After the selection of training site, several pixels have been assigned for different land use categories. Then the supervised classification has been applied over the assigned land use categories.

3 Results

The following section analyzes the spatiotemporal characteristics of rainfall for different seasons from 1980 to 2018 over Bhubaneswar city and its surroundings.

3.1 Temporal analysis of rainfall over Bhubaneswar

The wavelet coefficients obtained from CWT for precipitation at Bhubaneswar for the 1980–2018 period, seasonally. White contour lines enclose statistically significant wavelet power regions at a 95% confidence level in the time-frequency space (Fig. 4(a (i-iv))). The calculated wavelet power presented below the solid black line (COI) in Fig. 4(a) is considered unreliable due to its edge effects.

For the winter and post-monsoon season, significant inter-annual oscillations with periodicity as 1–130 years occurred from 1997 to 2003 over Bhubaneswar. Whereas, in pre-monsoon period significant inter-annual oscillations are within a more constrained 1–12 years' period, and more notably in the 1990s to 2000s period. For the

monsoon season, inter-annual oscillations are more pronounced at a 2–6 years' period. In other words, the monsoonal changes are most notable, followed by the pre-monsoon period. The winter and post-monsoon rainfall features do not show any notable change. Analysis of annual variation of seasonal maximum rainfall is shown in Fig. 2(b), which indicates an increasing trend in maximum seasonal rainfall for all seasons except for post-monsoon season across Bhubaneswar. The maximum seasonal rainfall showed an increase of 15.6 mm over 39 years for pre-monsoon season (0.4 mm per day in a season or year). In other studies, it is also analyzed that there is an increase in rainfall from last decade over the city (Li et al., 2020; Jiang et al., 2020). The rainfall in winter showed nearly half the increase as the pre-monsoon rains, while the monsoon rainfall showed even more muted change with only about 1 mm per decade. In post-monsoon season, the maximum seasonal rainfall showed a decrease of about 0.5 mm per decade. The MK significant test has been carried out for all the trend analysis. The p-value for these trends is 0.19, 0.15, 0.2, and 0.16 for winter, pre-monsoon, monsoon, and post-monsoon season are statically significant at 81%, 85%, 80%, and 84% significant level respectively.

Hourly rainfall across Bhubaneswar is analyzed next. The study period has been divided into two parts to examine how the peak rainfall hour changes with time. It is also observed from previous studies for different
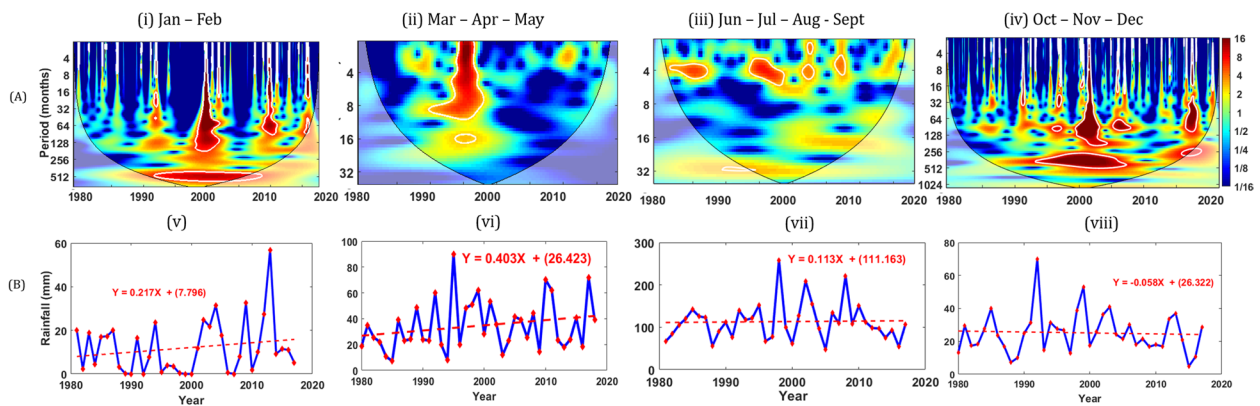
Fig. 4 A Wavelet transforms of monthly rainfall for (i) Jan – Feb, (ii) Mar-Apr-May, (iii) Jun-Jul-Aug-Sept, and (iv) Oct-Nov-Dec. The black line represents the cone-of-influence and white contours represent the 95% significance level; **B** Annual trend of seasonal maximum rainfall over Bhubaneswar from 1980 to 2018 for (v) Jan – Feb, (vi) Mar-Apr-May, (vii) Jun-Jul-Aug-Sept, and (viii) Oct-Nov-Dec.

urbanized cities (Zhu et al., 2019; Yuan et al., 2021). Wavelet transforms for 1980–1999 (first section) and 2000–2018 (second section) for different seasonal rainfall has been shown in Fig. 5(A) and (B), respectively. The analysis reveals a gradual but notable shift in the timing of the maximum rainfall. In the initial data period,

maximum rainfall generally occurs in the morning, i.e., around 8 am to 10 am. Whereas, during the second, it occurs during the afternoon, i.e., around 4 pm to 8 pm. This is more evident for pre-monsoon season. The initial rainfall data shows a noisy frequency, while the variability was more organized with a 1–3 h periodicity. For winter
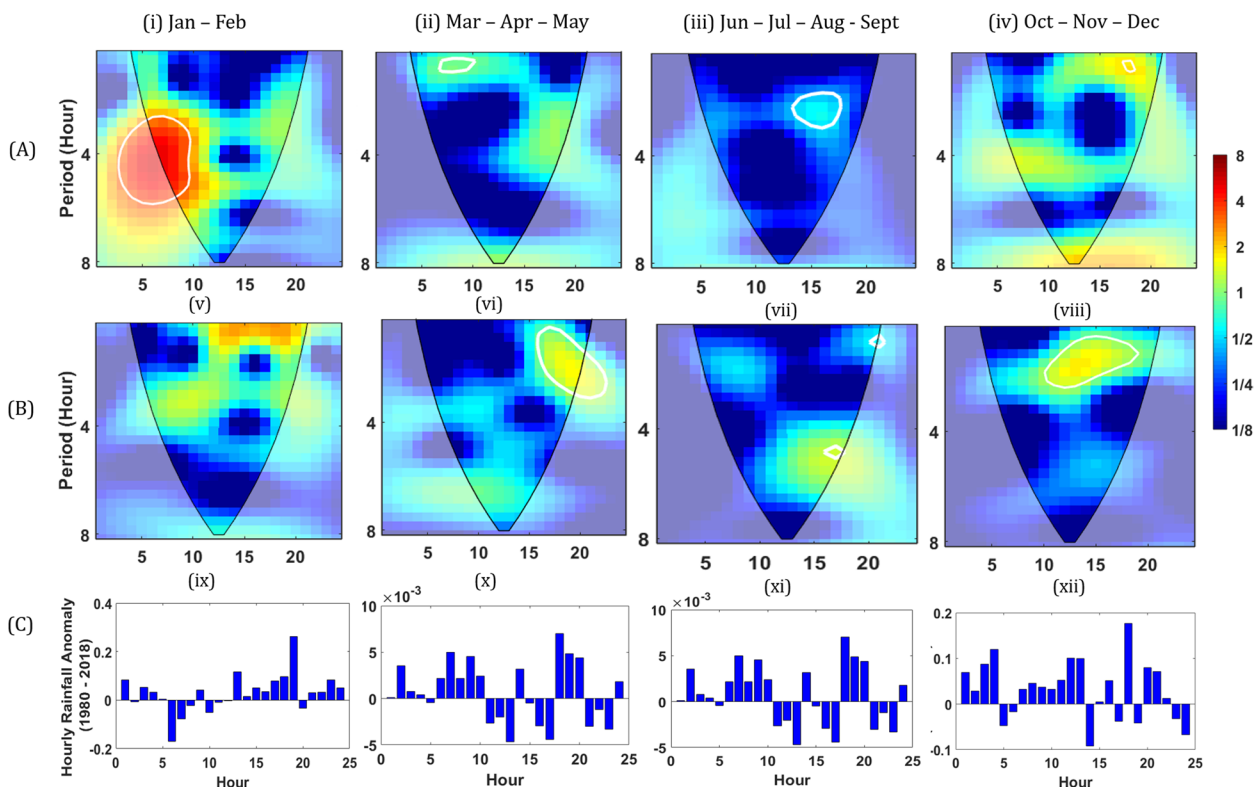

Fig. 5 A Wavelet transform of hourly rainfall during 1980–1999 time period for (i) Jan – Feb, (ii) Mar-Apr-May, (iii) Jun-Jul-Aug-Sept, and (iv) Oct-Nov-Dec; **B** is same as **A** but during 2000–2018 time period. The black line represents the cone-of-influence and white contours represent the 95% significance level; **C** Variation of hourly rainfall anomaly for 1980–2018 for (ix) Jan – Feb, (x) Mar-Apr-May, (xi) Jun-Jul-Aug-Sept, and (xii) Oct-Nov-Dec over Bhubaneswar

Swain *et al. Computational Urban Science*   (2023) 3:8

Page 8 of 14

season, maximum rainfall occurs during early morning, i.e. from 4 am to 10 am in the first section and in the second section it is around 3 pm to 5 pm (it is statistically insignificant). For the monsoon season, there is no detectable change in rainfall peak timing but the intensity showed increase in the second half of the data period. In the post-monsoon season, maximum rainfall occurs around or after 5 pm in the early half of the data period, and the rainfall occurs earlier i.e., around 11 am to 4 pm in the second section.

The hourly anomaly trend for 1980–2018 seasonal rainfall, and the analysis suggests an overall increase in rainfall intensity from midnight to late-evening over Bhubaneswar (Fig. 5(C)). It is also observed that maximum rainfall occurs from 5 pm to 8 pm during pre-monsoon season, and from 5 pm to 7 pm, from 6 pm to 8 pm, and around 6 pm during winter, monsoon, and post-monsoon seasons, respectively. This change in the rainfall timing is consistent for results from another urban center (Hyderabad, which is about 1000 km southwest) with similar urban sprawl in recent decades (Niyogi et al., 2020). The similarity of findings for Bhubaneswar, which has much more rapid urbanization and a dramatic change in the timing, is instructive. In that, the difference (or change) in rainfall timing over the city appears to be another signature of urban modification of rainfall – the first being the spatial change reported in the literature (Shepherd, 2005; Ntelekos et al., 2010; Routray et al, 2010; Liu & Niyogi, 2019).

3.2 Spatial analysis of rainfall over Bhubaneswar
Climatological mean rainfall during different seasons indicates that Bhubaneswar receives about 40–45 mm rains during pre-monsoon season which is maximum compared to other seasonal rainfall (Fig. 6(A)). Maximum rainfall occurs typically along the east side of the urbanized city for all seasons. The thunderstorm-centric east side of the city gets more rainfall (about 60 mm) than the west side of the city (about 30 mm) for pre-monsoon season. The distance of the rainfall maxima is approximately 40–50 km from the center of the city. Thus, there is a gradation in rainfall intensity from the west to the east side of the city, and climatologically, the rainfall difference is about 30 mm. That is, a factor of two increase in the rainfall east side of the city as compared to the west side is found. The rainfall maxima occur at ~50 km from the city center, which conforms to the summary of urban rainfall features reported in Liu and Niyogi (2019). Huff, 1975 did experiments in the St. Louis area, and they found that highest rain cell occurs over the urban region which is east side of the city. Further, the same has been confirmed in the recent study (Liu & Niyogi, 2019), that the east side of the storm is more impacted due to the anti-cyclonic circulation of low-pressure system over the city.

Trend analysis of pre-monsoonal rainfall over Bhubaneswar has been carried out with IMD gridded data and presented in Fig. 6(B). Results show that the rain over the city and along the east side of the city shows an increasing trend compared to the rainfall trend along the
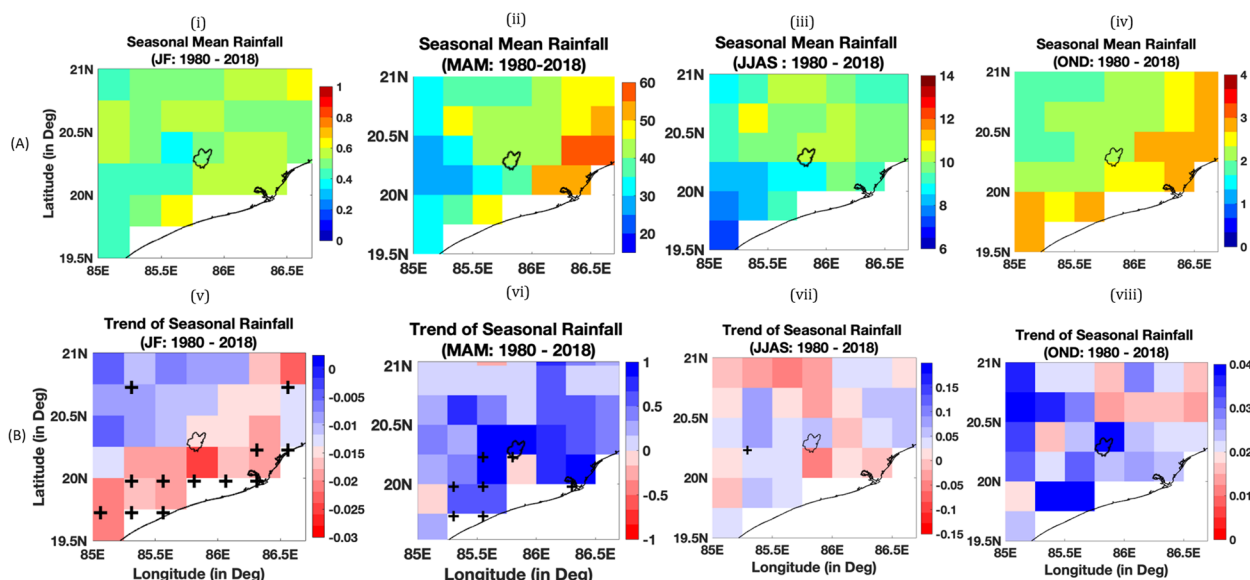

Fig. 6 Spatial distribution of **A** seasonal mean rainfall (black colour figure represents Bhubaneswar city boundary) for (i) Jan – Feb, (ii) Mar-Apr-May, (iii) Jun-Jul-Aug-Sept, and (iv) Oct-Nov-Dec; **B** is same as **A** but for trend of seasonal rainfall (black colour figure represents Bhubaneswar city boundary and black "+" shows the grid points having stastically significant rainfall)
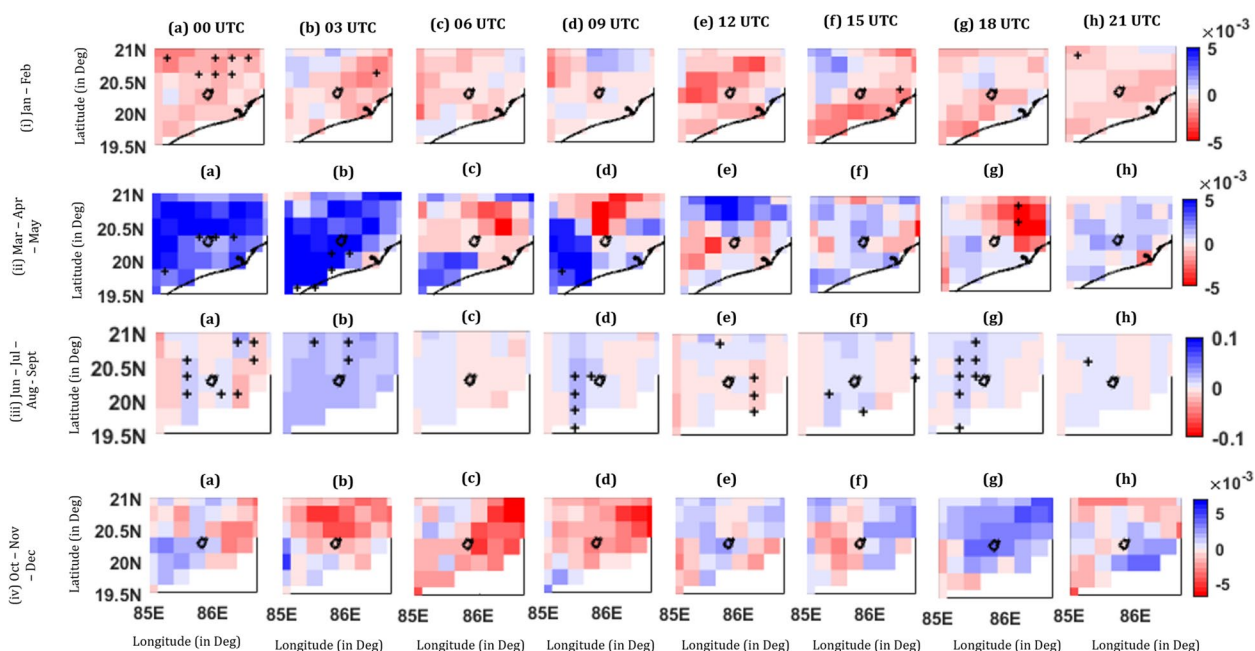
Fig. 7 Trend of 3-hourly rainfall during 1999–2018 year for (a) 00 UTC, (b) 03 UTC, (c) 06 UTC, (d) 09 UTC, (e) 12 UTC, (f) 15 UTC, (g)18 UTC, and (h) 21 UTC for (i) Jan – Feb, (ii) Mar-Apr-May, (iii) Jun-Jul-Aug-Sept, and (iv)Oct-Nov-Dec from TRMM gridded data (black colour figure represents Bhubaneswar city boundary and black "+" shows the grid points having stastically significant rainfall)

city's west side. But, during winter and post-monsoon season, rainfall along the west side of the city is showing an increasing trend compared to east side of the city. It is highlighted that the trends are relatively small, and the results should be considered as tentative.

For analyzing the spatiotemporal rainfall variation, 3-hourly rainfall data for 20-year period (1999–2018) using TRMM fields is presented in the supplementary Figs. 1–4. Considering the rapid urbanization rate noted for Bhubaneswar, the study period is divided into four epochs of 5-year intervals: (i) 1999–2003, (ii) 2004–2008, (iii) 2009–2013, and (iv) 2014–2018. During winter, the maximum rainfall is during 17.30 IST in the first interval, whereas more rainfall is occurring during 14.30 IST in recent times, i.e., the fourth interval. During pre-monsoon season, maximum rainfall is received around afternoon 14:30 IST in the first interval and during evening 17:30 IST in the second. The rainfall from past midnight (01.30 IST) to early morning (08.30 IST) has decreased from 1999 to 2018. In monsoon season, afternoon rainfall typically around 14:30 IST has decreased while the early evening 17:30 IST rainfall has increased over the time period. During post-monsoon season, maximum rainfall has occurred around 11:30 IST in the first interval and around 17:30 IST in second interval. This is summarized from the 3-hourly trend analysis of rainfall over Bhubaneswar (Fig. 7 (I-IV)). This hourly changes of rainfall in a day has also been found from Siswanto et al., 2016.

3.3 Changes in LULC over Bhubaneswar

The changes in the urbanized area from 1980 to 2019 over Bhubaneswar are examined (Fig. 8). The aim is to broadly assess the relation between urban sprawl and rainfall changes. Supervised classification of LULC map using ArcGIS leads to the quantification of change in LULC (Fig. 8(a)). The changes in the urban built-up area are shown in Fig. 8(b), which shows a dramatic increase in urban built-up area from 1980 to 2019. The urbanized area is concentrated over the central part of the city in 1980s, compared to the significant sprawl noted in the 2019 imagery. It is important to note that the urban growth noted over Bhubaneswar is possibly emblematic of the changes occurring across the different emerging cities of the world (Wang et al., 2006, Li et al., 2013, and Bechtel et al. 2017).

Then the population density for Bhubaneswar city has been plotted from 2000 (Fig. 8(c)). It shows an increasing trend in the urban built-up area, and population density over the city. Similar results have also been observed for Bhubaneswar city from 2003 to 2017 in Barik et al. (2019). The urban area is about $22.5\,km^2$ in 1980 and shows a more than five-fold increase to $122\,km^2$ in 2019. Thus, there is a change in about $100\,km^2$ in the last 39 years of the period. Spatial distribution of population density over Bhubaneswar suggests that the population density is increasing over the city and more is over east side of the city (Fig. 8(d)). It is concluded that the urban
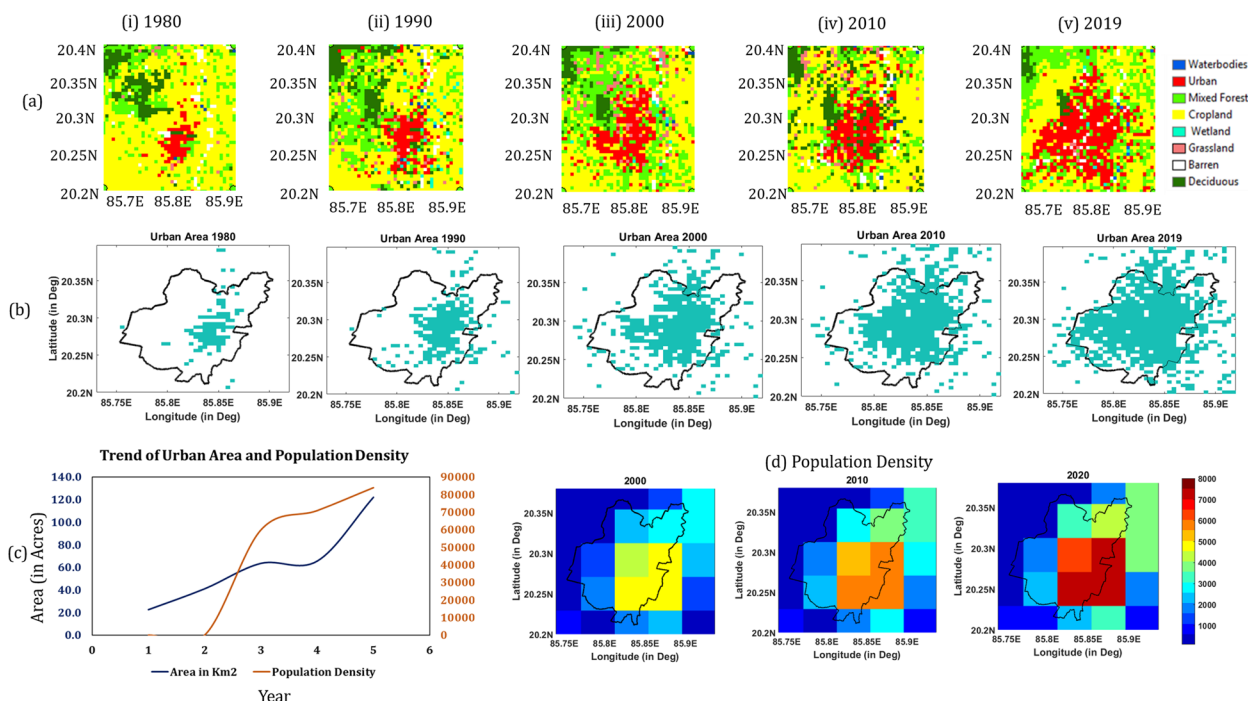
Fig. 8 **a** Classified LULC map for the study area, **b** spatial distribution of urban built-up area over the study area for 1980, 1990, 2000, 2010, and 2019 year, **c** Decadal variation of urban area (km²) and population density across Bhubaneswar, and **d** Spatial distribution of population density over Bhubaneswar for 2000, 2010, and 2020 year

area, rainfall, and population density are more along east side i.e. Rasulgarh (20.29 N, 85.86 E), Master Canteen (20.27 N, 85.84 E), and Rajmahal (20.26 N, 85.83 E) station points of Bhubaneswar city.

3.4 Change in rainfall over urban and peri-urban grid points

To clarify the association of rainfall, change with the increase in urbanization, the rainfall over urban and peri-urban grid points has been analyzed for different seasons (Fig. 9 (i-iv)). The difference in urban and peri-urban rainfall shows a modest but detectable increase from 1980 to 2019 period for all seasons. The increase in rainfall is more in monsoon season. For 1980s to 2000s the difference is negative or constant and does not show any notable impact of urbanization; whereas in recent period, the rainfall over the urban area is more compared to peri-urban regions; which is often associated with the urban heat island and rainfall impacts. The same has been observed in Li et al., 2020. Increase in urbanization increases surface temperature; which causes more surface evaporation, more local updraft over the region and intensify the rainfall intensity (Houston and Niyogi 2007).

3.5 Possible mechanism

A framework for the changes in rainfall due to urban intensification is presented here. The changes in the landscape characteristics due to urbanization lead to an increase in surface air temperature over the urban area relative to the peri-urban regions. This urban heat island (UHI) also leads to spatial gradients in the net radiation flux, as identified for the study region in Gogoi et al. (2019). The presence of UHI, especially in the pre-monsoon period, indicates a potential for enhanced vertical mixing and mesoscale circulation across the urban-rural interface. This favors a setup for moisture advection over the city. Surface winds upwind of the city are frequently altered (reduced) by urban roughness, and they may even accelerate downwind. This results in modified divergence and convergence patterns that are reflective of the microscale lateral pressure differential throughout the city transect and are visible along the city boundaries (Liu & Niyogi, 2019). The urban area likely provides sufficient energy to develop convective systems, elevating the clouds and rainfall water mixing ratio over the urban areas and thus causes more intensified rainfall (Simpson et al., 2008; Shem and Shepherd, 2009; Niyogi et al., 2011). The change in the timing of the rains
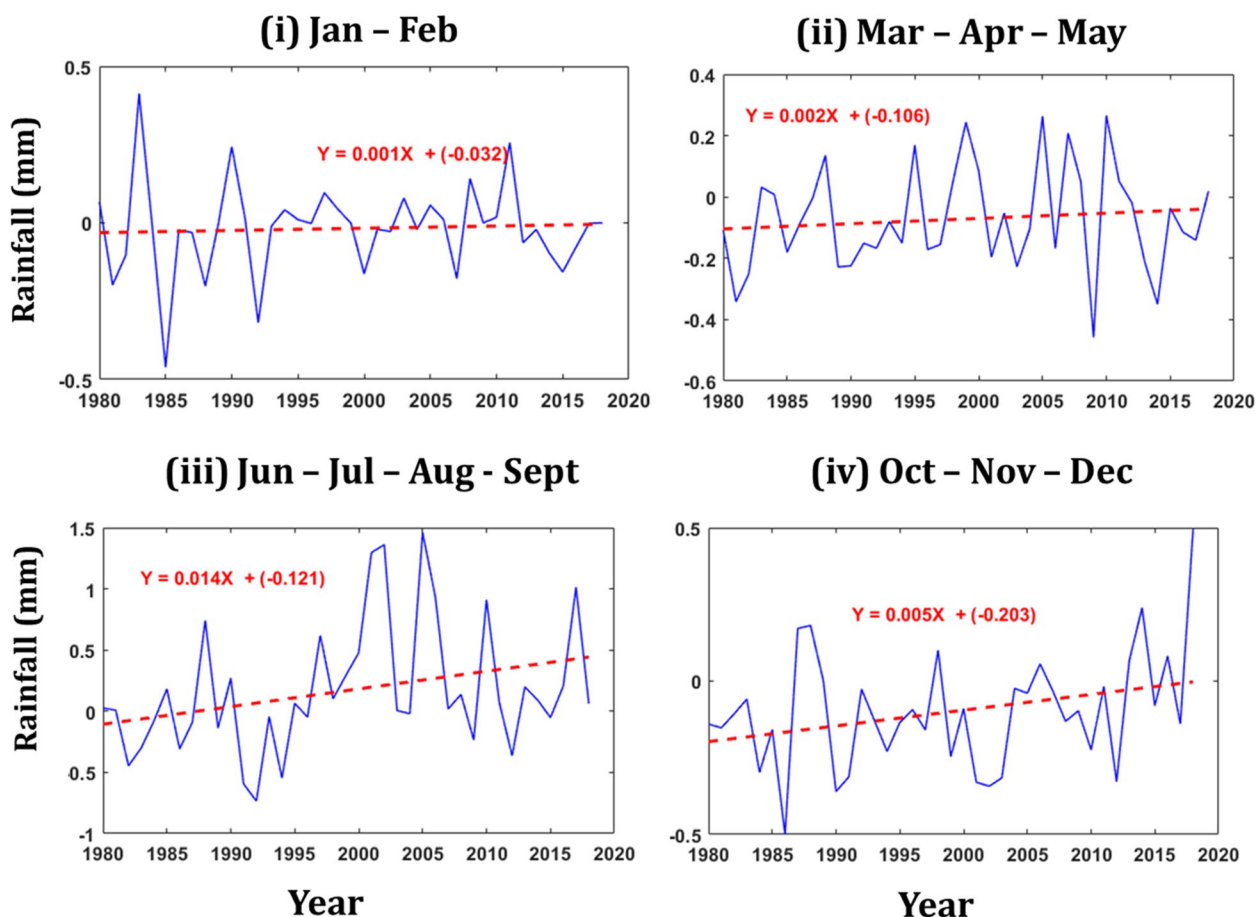
Fig. 9 Difference in rainfall over urban and per-urban grid-points during 1980–2019 for (i) Jan – Feb, (ii) Mar-Apr-May, (iii) Jun-Jul-Aug-Sept, and (iv) Oct-Nov-Dec

is further supported by the UHI feedback on the regional circulation and convection potential during the peak UHI conditions – late afternoon and evening. These features will be need to be evaluated in a future modeling study.

4 Conclusions

Spatiotemporal variation in four different seasonal rainfalls and the concurrent changes in LULC over Bhubaneswar city are analyzed. Study results are as follows.

Both wavelet and MK-trend analysis indicate a notable increase in rainfall intensity for different seasons except for post-monsoon season over Bhubaneswar. The maximum increasing amount is about 0.4 mm averaged over the city per season which occurs during premonsoon season. The analysis of hourly rainfall data indicates a change in both duration and magnitude of rainfall occurrence over the city for all seasons. Interestingly, there is a change in the timing of the rainfall with a decrease in the midnight to early-morning rains

and a corresponding increase in the late-afternoon to midnight rainfall from 1980 to 2018. In addition to the changes in the rainfall timing, there is an increasing trend of rainfall over the city and along the city's thunderstorm-relative east side compared to the west side of the city (which is at > 95% significant level).

A five-fold increase in urban built-up area over the study area is found over the last four decades. Thus, urbanization in the rapidly expanding city along the east coast of India has likely caused a notable change in the timing, magnitude, and rainfall location. The data trend is still weak but there are indicators that the transition will likely continue as the city expands even further into the coming decades. This research will shed light on how heavy precipitation in the urbanized metropolis of Odisha is affected by changes in urban infrastructure. The civil engineers, city planners, and urban water managers will benefit from this product in order to plan the city in consideration of future environmental effects of urbanization.

Swain *et al. Computational Urban Science*   (2023) 3:8

Page 12 of 14

Supplementary Information

The online version contains supplementary material available at https://doi.org/10.1007/s43762-023-00081-2.

> **Additional file 1: Supplementary Fig. 1.** 3-hourly mean rainfall for (A) 1980–2003, (B) 2004–2008, (C) 2009–2013, and (D) 2014–2018 for January–February. **Supplementary Fig. 2.** Same as supplementary fig. 1, but for March–April-May. **Supplementary Fig. 3.** Same as supplementary fig. 1, but for June–July-August-September. **Supplementary Fig. 4.** Same as supplementary fig. 1, but for October–November-December.

Code availability (software application or custom code)

Code will be available on request.

Authors' contributions

MS has done all the analysis and first draft writing of the manuscript. RRN, UCM, and DN have initialized the work and edited the manuscript. PG, AG, AK, and FC have supported to do the analysis. All the authors read and approved the final manuscript.

Availability of data and materials

TRMM rainfall data: https://giovanni.gsfc.nasa.gov/giovanni/
IMD rainfall data: http://dsp.imdpune.gov.in/
USGS data: https://landsat.gsfc.nasa.gov

Declarations

Competing interests

There is no conflict of interest.

References

Adarsh, S., & Reddy, J. M. (2015). Trend analysis of rainfall in four meteorological subdivisions of southern India using nonparametric methods and discrete wavelet transform. *International Journal of Climatology, 35*(6), 1107–1124. https://doi.org/10.1002/joc.4042

Arnfield, A. J. (2003). Two decades of urban climate research: A review of turbulence, exchanges of energy and water, and the urban heat island. *International Journal of Climatology: A Journal of the Royal Meteorological Society, 23*(1), 1–26.

Barik, A., Swain, D., & Vinoj, V. (2019). Rapid urbanization and associated impacts on land surface temperature changes over Bhubaneswar Urban District, India. *Environmental Monitoring and Assessment, 191*(3), 790. https://doi.org/10.1007/s10661-019-7699-2

Barsi, J. A., Hook, S. J., Schott, J. R., Raqueno, N. G., & Markham, B. L. (2007). Landsat-5 thematic mapper thermal band calibration update. *IEEE Geoscience and Remote Sensing Letters, 4*(4), 552–555. https://doi.org/10.1109/LGRS.2007.896322

Bechtel, B., Demuzere, M., Sismanidis, P., Fenner, D., Brousse, O., Beck, C., Van Coillie, F., Conrad, O., Keramitsoglou, I., Middel, A. and Mills, G., (2017). Quality of crowdsourced data on urban morphology—the human influence experiment (HUMINEX). *Urban Science, 1*(2), 15. https://doi.org/10.1111/j.1752-1688.1988.tb00904.x

Berryman, D., Bobee, B., Cluis, D., & Haemmerli, J. (1988). Nonparametric tests for trend detection in water quality time series. Water Resources Bulletin, 24, 545–556. https://doi.org/10.1111/j.1752-1688.1988.tb00904.x

Bhattacharya, S., Rathi, S., Patro, S. A., & Tepa, N. (2015). *Reconceptualising smart cities: A reference framework for India*. CSTEP-Report-2015-03.

Birsan, M. V., Molnar, P., Burlando, P., & Pfaundler, M. (2005). Streamflow trends in Switzerland. *Journal of Hydrology, 314*(1–4), 312–329. https://doi.org/10.1016/j.jhydrol.2005.06.008

Bisht, D. S., Chatterjee, C., Raghuwanshi, N. S., & Sridhar, V. (2018). Spatio-temporal trends of rainfall across Indian river basins. *Theoretical and Applied Climatology, 132*(1–2), 419–436. https://doi.org/10.1007/s00704-017-2095-8

Buishand, T. A. (1979). Urbanization and changes in precipitation, a statistical approach. *Journal of Hydrology, 40*(3–4), 365–375. https://doi.org/10.1016/0022-1694(79)90039-8

Burian, S. J., & Shepherd, J. M. (2005). Effect of urbanization on the diurnal rainfall pattern in Houston. *Hydrological Processes: An International Journal, 19*(5), 1089–1103. https://doi.org/10.1002/hyp.5647

Census of India, Odisha State. (2011). *Office of the Registrar General and Census Commissioner, India 2/a, man Singh road, New Delhi-110011, India*.

Center for International Earth Science Information Network (CIESIN), Columbia University. (2018). *Documentation for the gridded population of the world, version 4 (GPWv4), revision 11 data sets*. NASA Socioeconomic Data and Applications Center (SEDAC).

Chen, T. C., Wang, S. Y., & Yen, M. C. (2007). Enhancement of afternoon thunderstorm activity by urbanization in a valley: Taipei. *Journal of Applied Meteorology and Climatology, 46*(9), 1324–1340. https://doi.org/10.1175/JAM2526.1

Choudhury, A., Sirsikar, D. Y., & Pati, D. (2011). *Ground water scenario in Bhubaneswar city, Odisha* India water week 2011: Ground water Scenario in Indian cities.

Daubechies, I. (1990). *The wavelet transform, time-frequency localization and signal analysis* (pp. 442–486). Princeton University Press. https://doi.org/10.1515/9781400827268.442

Dimri, A.P. and Niyogi, D., (2013). Regional climate model application at subgrid scale on Indian winter monsoon over the western Himalayas. *International Journal of Climatology, 33*(9), 2185-2205. https://doi.org/10.1016/j.apgeog.2008.12.005.

Dewan, A. M., & Yamaguchi, Y. (2009). Land use and land cover change in greater Dhaka, Bangladesh: Using remote sensing to promote sustainable urbanization. *Applied Geography, 29* (3), 390–401. https://doi.org/10.1016/j.apgeog.2008.12.005

Eastman, J. R. (2003). *IDRISI Kilimanjaro: Guide to GIS and image processing*.

Fu, G., Chen, S., Liu, C., & Shepard, D. (2004). Hydro-climatic trends of the Yellow River basin for the last 50 years. *Climatic Change, 65*(1–2), 149–178. https://doi.org/10.1023/B:CLIM.0000037491.95395.bb

Gogoi, P. P., Vinoj, V., Swain, D., Roberts, G., Dash, J., & Tripathy, S. (2019). Land use and land cover change effect on surface temperature over eastern India. *Scientific Reports, 9*(1), 1–10. https://doi.org/10.1038/s41598-019-45213-z

Gu, X., Sun, H., Zhang, Y., Yu, Z., & Zhu, J. (2020). Multiple wavelet coherence to evaluate local multivariate relationships in a groundwater system. *Groundwater., 59*(3), 443–452. https://doi.org/10.1111/gwat.13068

Gupta, K. (2020). Challenges in developing urban flood resilience in India. *Philosophical Transactions of the Royal Society A, 378*(2168), 20190211. https://doi.org/10.1098/rsta.2019.0211

Swain *et al. Computational Urban Science*   (2023) 3:8

Page 13 of 14

Gupta, M. M., Gupta, A., & Kumar, P. (2018). Urbanization and biodiversity of arbuscular mycorrhizal fungi: The case study of Delhi, India. *Revista de Biología Tropical, 66*(4), 1547–1558. https://doi.org/10.15517/rbt.v66i4.33216

Helsel, D. R., & Hirsch, R. M. (1992). *Statistical methods in water resources (Vol. 49)*. Elsevier.Houston, A.L. and Niyogi, D., (2007). The sensitivity of convective initiation to the lapse rate of the active cloud-bearing layer. Monthly Weather Review,135(9), 3013-3032.

Houston, A.L. and Niyogi, D., (2007). The sensitivity of convective initiation to the lapse rate of the active cloud-bearing layer. *Monthly Weather Review, 135*(9), 3013-3032.

Huff, F. A. (1975). Urban effects on the distribution of heavy convective rainfall. *Water Resources Research, 11*(6), 889–896.

Huffman, G. J., Bolvin, D. T., & Nelkin, E. J. (2015). Integrated multi-satellite retrievals for GPM (IMERG) technical documentation. *NASA/GSFC Code, 612*(47), 2019.

Jain, M., Dimri, A. P., & Niyogi, D. (2016). Urban sprawl patterns and processes in Delhi from 1977 to 2014 based on remote sensing and spatial metrics approaches. *Earth Interactions, 20*(14), 1–29. https://doi.org/10.1175/EI-D-15-0040.1

Jha, M. K., & Singh, A. K. (2013). Trend analysis of extreme runoff events in major river basins of peninsular Malaysia. *International Journal of Water, 7*(1–2), 142–158. https://doi.org/10.1504/IJW.2013.051995

Jiang, X., Luo, Y., Zhang, D. L., & Wu, M. (2020). Urbanization enhanced summertime extreme hourly precipitation over the Yangtze River Delta. *Journal of Climate, 33*(13), 5809–5826.

Kendall, M. G. (1948). *Rank correlation methods*.

Kishtawal, C. M., Niyogi, D., Tewari, M., Pielke, R. A., & Shepherd, J. M. (2010). Urbanization signature in the observed heavy rainfall climatology over India. *International Journal of Climatology, 30*(13), 1908–1916. https://doi.org/10.1002/joc.2044

Kumar, P. (1996). Role of coherent structures in the stochastic-dynamic variability of precipitation. *Journal of Geophysical Research-Atmospheres, 101*(D21), 26393–26404. https://doi.org/10.1029/96JD01839.

Kumar, S., Dirmeyer, P.A., Merwade, V., DelSole, T., Adams, J.M. and Niyogi, D., (2013). Land use/cover change impacts in CMIP5 climate simulations: A new methodology and 21st century challenges. *Journal of Geophysical Research: Atmospheres, 118*(12), 6337-6353.

Li, C., Li, J., & Wu, J. (2013). Quantifying the speed, growth modes, and landscape pattern changes of urbanization: A hierarchical patch dynamics approach. *Landscape Ecology, 28*(10), 1875–1888. https://doi.org/10.1007/s10980-013-9933-6

Li, Y., Fowler, H. J., Argüeso, D., Blenkinsop, S., Evans, J. P., Lenderink, G., Yan, X., Guerreiro, S. B., Lewis, E., & Li, X.-F. (2020). Strong intensification of hourly rainfall extremes by urbanization. *Geophysical Research Letters, 47*(14), e2020GL088758.

Liang, P., Ding, Y. H., He, J. H., & Tang, X. (2011). Study of relationship between urbanization speed and change of spatial distribution of rainfall over Shanghai. *Journal of Tropical Meteorology, 27*(4), 475–483. https://doi.org/10.1016/j.quaint.2012.01.033

Ling, H., Xu, H., Fu, J., Zhang, Q., & Xu, X. (2012). Analysis of temporal-spatial variation characteristics of extreme air temperature in Xinjiang, China. *Quaternary International, 282*, 14–26.

Liu, J., & Niyogi, D. (2019). Meta-analysis of urbanization impact on rainfall modification. *Scientific Reports, 9*(1), 1–14. https://doi.org/10.1038/s41598-019-42494-2

Lorenz, J. M., Kronenberg, R., Bernhofer, C., & Niyogi, D. (2019). Urban rainfall modification: Observational climatology over Berlin, Germany. *Journal of Geophysical Research-Atmospheres, 124*(2), 731–746.

Mann, H. B. (1945). Nonparametric tests against trend. *Econometrica: Journal of the Econometric Society*, 245–259. https://doi.org/10.2307/1907187

Meyers, S. D., Kelly, B. G., & O'Brien, J. J. (1993). An introduction to wavelet analysis in oceanography and meteorology: With application to the dispersion of Yanai waves. *Monthly Weather Review, 121*(10), 2858–2866. https://doi.org/10.1175/1520-0493(1993)121<2858:AITWAI>2.0.CO;2

Modarres, R., & Sarhadi, A. (2009). Rainfall trends analysis of Iran in the last half of the twentieth century. *Journal of Geophysical Research-Atmospheres, 114*(D3). https://doi.org/10.1029/2008JD010707

Mohanty, U. C., Mohapatra, M., Singh, O. P., Bandyopadhyay, B. K., & Rathore, L. S. (2013). Monitoring and prediction of tropical cyclones in the Indian Ocean and climate change. *Springer Science & Business Media*. https://doi.org/10.1007/978-94-007-7720-0

National Research Council. (2010). *Pathways to urban sustainability: Research and development on urban systems: Summary of a workshop*. National Academies Press.

Niyogi, D., Lei, M., Kishtawal, C., Schmid, P., & Shepherd, M. (2017). Urbanization impacts on the summer heavy rainfall climatology over the eastern United States. *Earth Interactions, 21*(5), 1–17.

Niyogi, D., Osuri, K. K., Busireddy, N. K. R., & Nadimpalli, R. (2020). Timing of rainfall occurrence altered by urban sprawl- a case study over Hyderabad city of India. *Urban Climate, 33*. https://doi.org/10.1016/j.uclim.2020.100643

Niyogi, D., Pyle, P., Lei, M., Arya, S. P., Kishtawal, C. M., Shepherd, M., Chen, F., & Wolfe, B. (2011). Urban modification of thunderstorms: An observational storm climatology and model case study for the Indianapolis urban region. *Journal of Applied Meteorology and Climatology, 50*(5), 1129–1144. https://doi.org/10.1175/2010JAMC1836.1

Ntelekos, A. A., Oppenheimer, M., Smith, J. A., & Miller, A. J. (2010). Urbanization, climate change and flood policy in the United States. *Climatic Change, 103*(3), 597–616.

Pai, D. S., Sridhar, L., Rajeevan, M., Sreejith, O. P., Satbhai, N. S., & Mukhopadhyay, B. (2014). Development of a new high spatial resolution (0.25 × 0.25) long period (1901–2010) daily gridded rainfall data set over India and its comparison with existing data sets over the region. *Mausam, 65*(1), 1–18.

Pal, L., Ojha, C. S. P., Chandniha, S. K., & Kumar, A. (2019). Regional scale analysis of trends in rainfall using nonparametric methods and wavelet transforms over a semi-arid region in India. *International Journal of Climatology, 39*(5), 2737–2764. https://doi.org/10.1002/joc.5985

Panda, D. K., Mishra, A., Kumar, A., Mandal, K. G., Thakur, A. K., & Srivastava, R. C. (2014). Spatiotemporal patterns in the mean and extreme temperature indices of India, 1971–2005. *International Journal of Climatology, 34*(13), 3585–3603. https://doi.org/10.1002/joc.3931

Pandey, S., Scharf, B. W., & Mohanti, M. (2014). Palynological studies on mangrove ecosystem of the Chilka lagoon, east coast of India during the last 4165 yrs BP. *Quaternary International, 325*, 126–135.

Partal, T., & Küçük, M. (2006). Long-term trend analysis using discrete wavelet components of annual precipitations measurements in Marmara region (Turkey). *Physics and Chemistry of the Earth, Parts A/B/C, 31*(18), 1189–1200. https://doi.org/10.1016/j.pce.2006.04.043

Pathy, A. C., & Panda, G. K. (2012). Modeling urban growth in Indian situation- a case study of Bhubaneswar city. *International Journal of Scientific and Engineering Research, 3*(6), 1–7.

Pielke Sr., R. A., Pitman, A., Niyogi, D., Mahmood, R., McAlpine, C., Hossain, F., Goldewijk, K. K., Nair, U., Betts, R., Fall, S., & Reichstein, M. (2011). Land use/land cover changes and climate: Modeling analysis and observational evidence. *Wiley Interdisciplinary Reviews: Climate Change, 2*(6), 828–850. https://doi.org/10.1002/wcc.144

Rathinasamy, M., Agarwal, A., Sivakumar, B., Marwan, N., & Kurths, J. (2019). Wavelet analysis of precipitation extremes over India and teleconnections to climate indices. *Stochastic Environmental Research and Risk Assessment, 33*(11–12), 2053–2069. https://doi.org/10.1007/s00477-019-01738-3

Routray, A., Mohanty, U.C., Rizvi, S.R.H., Niyogi, D., Osuri, K.K. and Pradhan, D., (2010). Impact of Doppler weather radar data on numerical forecast of Indian monsoon depressions. *Quarterly Journal of the Royal Meteorological Society, 136*(652), 1836-1850.

Sang, Y. F. (2013). A review on the applications of wavelet transform in hydrology time series analysis. *Atmospheric Research, 122*, 8–15. https://doi.org/10.1016/j.atmosres.2012.11.003

Santos, C. A. G., Galvao, C. O., Trigo, R. M., & Servat, E. (2003). Rainfall data analysis using wavelet transform. *International Association of Hydrological Sciences, 278*, 195–201.

Seto, K. C., & David, S. (2010). Interactions between urbanization and global environmental change. *Current Opinion in Environmental Sustainability, 2*(3), 127–128. https://doi.org/10.1016/j.cosust.2010.07.003

Shem, W., & Shepherd, M. (2009). On the impact of urbanization on summertime thunderstorms in Atlanta: Two numerical model case studies. *Atmospheric Research, 92*(2), 172–189. https://doi.org/10.1016/j.atmosres.2008.09.013

Swain *et al. Computational Urban Science*　　　(2023) 3:8

Page 14 of 14

Shepherd, J. M. (2005). A review of current investigations of urban-induced rainfall and recommendations for the future. *Earth Interactions, 9*(12), 1–27. https://doi.org/10.1175/EI156.1

Shepherd, J. M., Pierce, H., & Negri, A. J. (2002). Rainfall modification by major urban areas: Observations from space borne rain radar on the TRMM satellite. *Journal of Applied Meteorology, 41*(7), 689–701.

Shi, P., Bai, X., Kong, F., Fang, J., Gong, D., Zhou, T., Guo, Y., Liu, Y., Dong, W., Wei, Z., & He, C. (2017). Urbanization and air quality as major drivers of altered spatiotemporal patterns of heavy rainfall in China. *Landscape Ecology, 32*(8), 1723–1738. https://doi.org/10.1007/s10980-017-0538-3

Shiau, J. T., & Chiu, Y. F. (2019). Wavelet-based detection of time-frequency changes for monthly rainfall and SPI series in Taiwan. *Asia-Pacific Journal of Atmospheric Sciences, 55*(4), 657–667. https://doi.org/10.1007/s13143-019-00118-9

Simpson, M., Raman, S., Suresh, R., & Mohanty, U. C. (2008). Urban effects of Chennai on sea breeze induced convection and precipitation. *Journal of Earth System Science, 117*(6), 897–909. https://doi.org/10.1007/s12040-008-0075-1

Singh, J., Karmakar, S., Paimazumder, D., Ghosh, S., & Niyogi, D. (2020). Urbanization alters rainfall extremes over the contiguous United States. *Environmental Research Letters*. https://doi.org/10.1088/1748-9326/ab8980

Singh, J., Vittal, H., Karmakar, S., Ghosh, S., & Niyogi, D. (2016). Urbanization causes nonstationarity in Indian summer monsoon rainfall extremes. *Geophysical Research Letters, 43*(21), 11–26. https://doi.org/10.1002/2016GL071238

Singh, P., Kumar, V., Thomas, T., & Arora, M. (2008). Changes in rainfall and relative humidity in river basins in northwest and Central India. *Hydrological Processes: An International Journal, 22*(16), 2982–2992. https://doi.org/10.1002/hyp.6871

Siswanto, S., van Oldenborgh, G. J., van der Schrier, G., Jilderda, R., & van den Hurk, B. (2016). Temperature, extreme precipitation, and diurnal rainfall changes in the urbanized Jakarta city during the past 130 years. *International Journal of Climatology, 36*(9), 3207–3225. https://doi.org/10.1002/joc.4548

Solecki, W., Seto, K. C., & Marcotullio, P. J. (2013). It's time for an urbanization science. *Environment: Science and Policy for Sustainable Development, 55*(1), 12–17. https://doi.org/10.1080/00139157.2013.748387

Suhaila, J., & Jemain, A. A. (2009). A comparison of the rainfall patterns between stations on the east and the west coasts of peninsular Malaysia using the smoothing model of rainfall amounts. *Meteorological Applications, 16*(3), 391–401. https://doi.org/10.1002/met.137

Swain, D., Roberts, G. J., Dash, J., Lekshmi, K., Vinoj, V., & Tripathy, S. (2017). Impact of rapid urbanization on the city of Bhubaneswar, India. *Proceedings of the National Academy of Sciences, India Section A: Physical Sciences, 87*(4), 845–853. https://doi.org/10.1007/s40010-017-0453-7

Tan, X., Gan, T. Y., & Shao, D. (2016). Wavelet analysis of precipitation extremes over Canadian ecoregions and teleconnections to large-scale climate anomalies. *Journal of Geophysical Research-Atmospheres, 121*(24), 14–469. https://doi.org/10.1002/2016JD025533

Thandar, S. (2012). Analysis of Spatio-temporal changes of urban land use using remote sensing and GIS: A case study of Bhubaneswar City, Odisha. *Dagon University Research Journal, 4*, 19–29.

Torrence, C., & Compo, G. P. (1998). A practical guide to wavelet analysis. *Bulletin of the American Meteorological Society, 79*, 61–78. https://doi.org/10.1175/1520-0477(1998)079<0061:APGTWA>2.0.CO;2

Wang, B., & Wang, Y. (1996). Temporal structure of the southern oscillation as revealed by waveform and wavelet analysis. *Journal of Climate, 9*(7), 1586–1598. https://doi.org/10.1175/1520-0442(1996)009<1586:TSOTSO>2.0.CO;2

Wang, B., Zhang, M., Wei, J., Wang, S., Li, X., Li, S., Zhao, A., Li, X., & Fan, J. (2013). Changes in extreme precipitation over Northeast China, 1960–2011. *Quaternary International, 298*, 177–186. https://doi.org/10.1016/j.quaint.2013.01.025

Wang, Y. J., Li, J. X., Wu, J. P., & Song, Y. (2006). Landscape pattern changes in urbanization of Pudong New District, Shanghai. *The Journal of Applied Ecology, 17*(1), 36–40.

Wei, S., Song, J., & Khan, N. I. (2012). Simulating and predicting river discharge time series using a wavelet-neural network hybrid modelling approach. *Hydrological Processes, 26*(2), 281–296. https://doi.org/10.1002/hyp.8227

Wen, J., Chen, J., Lin, W., Jiang, B., Xu, S., & Lan, J. (2020). Impacts of anthropogenic heat flux and urban land use change on frontal rainfall near coastal regions: A case study of a rainstorm over the Pearl River Delta, South China. *Journal of Applied Meteorology and Climatology, 59*(3), 363–379. https://doi.org/10.1175/JAMC-D-18-0296.1

Weng, H., & Lau, K. M. (1994). Wavelets, period doubling, and time–frequency localization with application to organization of convection over the tropical western Pacific. *Journal of the Atmospheric Sciences, 51*(17), 2523–2541. https://doi.org/10.1175/1520-0469(1994)051<2523:WPDATL>2.0.CO;2

Yang, L., Tian, F., & Niyogi, D. (2015). A need to revisit hydrologic responses to urbanization by incorporating the feedback on spatial rainfall patterns. *Urban Climate, 12*, 128–140. https://doi.org/10.1016/j.uclim.2015.03.001

Yang, P., Ren, G., & Yan, P. (2017). Evidence for a strong association of short-duration intense rainfall with urbanization in the Beijing urban area. *Journal of Climate, 30*(15), 5851–5870. https://doi.org/10.1175/JCLI-D-16-0671.1

Yuan, Y., Zhai, P., Chen, Y., & Li, J. (2021). Hourly extreme precipitation changes under the influences of regional and urbanization effects in Beijing. *International Journal of Climatology, 41*(2), 1179–1189.

Yue, S., Pilon, P., & Phinney, B. O. B. (2003). Canadian streamflow trend detection: Impacts of serial and cross-correlation. *Hydrological Sciences Journal, 48*(1), 51–63. https://doi.org/10.1623/hysj.48.1.51.43478

Zhang, X., et al. (2019). Urban drought challenge to 2030 sustainable development goals. *Science of the Total Environment, 693*, 133536.

Zhi-Hong, J., Yang, L., & Dan-Lian, H. (2016). Impact of urbanization in different regions of eastern China on precipitation and its uncertainty. *Journal of Tropical Meteorology, 22*(3), 382.

Zhu, X., Zhang, Q., Sun, P., Singh, V. P., Shi, P., & Song, C. (2019). Impact of urbanization on hourly precipitation in Beijing, China: Spatiotemporal patterns and causes. *Global and Planetary Change, 172*, 307–324. https://doi.org/10.1016/j.gloplacha.2018.10.018

Publisher's Note